Hindawi Publishing Corporation
Journal of Chemistry
Volume 2015, Article ID 269387, 10 pages
http://dx.doi.org/10.1155/2015/269387

Research Article

Characterization, Dissolution, and Solubility of Lead Hydroxypyromorphite [$Pb_5(PO_4)_3OH$] at 25–45°C

Yinian Zhu,[1] Zongqiang Zhu,[1] Xin Zhao,[2] Yanpeng Liang,[1] and Yanhua Huang[1]

[1]*College of Environmental Science and Engineering, Guilin University of Technology, Guilin 541004, China*
[2]*College of Light Industry and Food Engineering, Guangxi University, Nanning 530004, China*

Correspondence should be addressed to Yinian Zhu; zhuyinian@glut.edu.cn and Zongqiang Zhu; zhuzongqiang@glut.edu.cn

Received 28 February 2015; Revised 16 April 2015; Accepted 17 April 2015

Academic Editor: Yuangen Yang

Dissolution of the hydroxypyromorphite [lead hydroxyapatite, $Pb_5(PO_4)_3OH$] in HNO_3 solution (pH = 2.00), ultrapure water (pH = 5.60), and NaOH solution (pH = 9.00) was experimentally studied at 25°C, 35°C, and 45°C. The XRD, FT-IR, and FE-SEM analyses indicated that the hydroxypyromorphite solids were observed to have indistinguishable change during dissolution. For the hydroxypyromorphite dissolution in aqueous acidic media at initial pH 2.00 and 25°C, the aqueous phosphate concentrations rose quickly and reached the peak values after 1 h dissolution, while the aqueous lead concentrations rose slowly and reached the peak values after 1440 h. The solution Pb/P molar ratio increased constantly from 1.10 to 1.65 near the stoichiometric ratio of 1.67 to 209.85~597.72 and then decreased to 74.76~237.26 for the dissolution at initial pH 2.00 and 25°C~45°C. The average K_{sp} values for $Pb_5(PO_4)_3OH$ were determined to be $10^{-80.77}$ ($10^{-80.57}$–$10^{-80.96}$) at 25°C, $10^{-80.65}$ ($10^{-80.38}$–$10^{-80.99}$) at 35°C, and $10^{-79.96}$ ($10^{-79.38}$–$10^{-80.71}$) at 45°C. From the obtained solubility data for the dissolution at initial pH 2.00 and 25°C, the Gibbs free energy of formation [ΔG_f^o] for $Pb_5(PO_4)_3OH$ was calculated to be −3796.71 kJ/mol (−3795.55~ −3797.78 kJ/mol).

1. Introduction

The calcium in hydroxyapatite [$Ca_5(PO_4)_3OH$, Ca-HAP] can be substituted by different divalent cations such as Pb^{2+} [1–6]. When the toxic lead ions, which may be found in surface and underground waters, are taken into animals, it is possible that they concentrate in animals' hard tissues through the substitution of Pb^{2+} for Ca^{2+} and form the Pb-Ca hydroxyapatite solid solution with vital calcium hydroxyapatite and can finally cause many bone diseases, such as osteoporotic processes and dental caries [1, 7–9]. The synthetic or natural calcium hydroxyapatite (Ca-HAP) from different sources can be used to remove toxic lead ions from industrial wastewaters [9–11]. The reaction of the solid Ca-HAP with lead ions resulted in the forming of hydroxypyromorphite [lead hydroxyapatite, $Pb_5(PO_4)_3OH$, Pb-HAP], which could include the fact that the dissolution of hydroxyapatite is followed with the forming of hydroxypyromorphite [12–15]. Lead apatite can form quickly in the presence of adequate phosphate and lead ions. It is recognized as the most stable lead form under a wide variety of environmental conditions. In situ immobilization of lead-contaminated systems with phosphates is now considered to be an appropriate and cost-effective technology [16, 17].

The substitution of Ca^{2+} in calcium hydroxyapatite by toxic Pb^{2+} is of considerable importance in a great variety of research areas [5, 11], which therefore needs an understanding of the essential physicochemical properties, especially the dissolution mechanism, solubility, and stability of hydroxypyromorphite under different conditions. Even though a lot of experiments on the dissolution mechanism and kinetics of natural and synthetic apatite samples in pure water and acidic and alkali solutions have been conducted [18–24], many of them have been only focused on calcium hydroxyapatite and fluorapatite. Unfortunately, the literature data on the thermochemical properties of hydroxypyromorphite is very sparse, which are required to clarify the behavior of hydroxypyromorphite in water environments, although its dissolution and following release of the component from solid to solution play a significant role in the cycling of lead and phosphate [24].

A unique K_{sp} value for hydroxypyromorphite (Pb-HAP) has been reported to be nearly $10^{-76.8}$ [24, 25], which has been also adopted in many subsequent studies, such as in the minteq.v4.dat database [26]. But this value for the solid phase [$Pb_5(PO_4)_3OH$] was not measured directly through precipitation or dissolution experiment; that is, it was calculated from an investigation of the hydrolysis of secondary and tertiary lead orthophosphates [$PbHPO_4$, $Pb_3(PO_4)_2$] in the pH range 3.00~10.00. In this study, lead hydroxypyromorphite was assumed to be a product in the alkaline hydrolysis of secondary lead orthophosphate without characterizing different phases of the solid [24]. In addition, the dissolution kinetics of hydroxypyromorphite has never been studied.

Thus, the lead hydroxypyromorphite (Pb-HAP) was first synthesized by precipitation method and examined by XRD, FT-IR, and FE-SEM in this work, and then its mechanism and dissolution rate were investigated at initial pH 2.00~9.00 and 25~45°C. Moreover, the aqueous concentrations were used to estimate the solubility product and free energy of forming for hydroxypyromorphite.

2. Experimental Methods

2.1. Solid Preparation and Characterization. The pure lead hydroxypyromorphite (Pb-HAP) solid sample was prepared by precipitation as the following reaction: $5\,Pb^{2+} + 3PO_4^{3-} + OH^- = Pb_5(PO_4)_3OH$ [27]. The synthetic procedure was dependent on 250 mL of 0.4 mol/L Pb solution that was first prepared by dissolving lead acetate hydrate [$Pb(CH_3COO)_2{\cdot}H_2O$, analytical grade] in ultrapure water. The Pb solution was then mixed with 250 mL 4.4 mol/L CH_3COONH_4 buffer solution in a 1 L polypropylene vessel. After that, 500 mL 0.12 mol/L $NH_4H_2PO_4$ solution was rapidly added to the vessel with stirring, resulting in white suspension. The suspension was adjusted to pH 7.50 by adding NH_4OH solution, stirred for 10 min at room temperature, and aged at 100°C for 48 h. The obtained precipitate was then settled, washed carefully using ultrapure water, and finally dried in an oven at 70°C for 16 h.

10 mg of the obtained hydroxypyromorphite solid was first dissolved in 20 mL of 1 mol/L nitric acid solution and diluted to 100 mL with ultrapure water. The Pb and P concentrations were then determined by the inductively coupled plasma-optical emission spectrometer (ICP-OES, PE Optima 7000DV). The prepared solid was also examined by the powder X-ray diffractometer (XRD, X'Pert PRO) using Cu Kα radiation (40 kV and 40 mA) at a scanning rate of 0.10°/min within a 2θ range 10~80° and then identified crystallographically via comparing the obtained XRD pattern with the ICDD reference code 01-087-2477 for lead hydroxyapatite. The solid was also investigated in KBr pellets within 4000~400 cm^{-1} using the Fourier transform infrared spectrophotometer (FT-IR, Nicolet Nexus 470). The morphology was scanned by the field emission-scanning electron microscope (FE-SEM, Hitachi S-4800).

2.2. Dissolution Experiments. 2.0 g of the synthetical hydroxypyromorphite solid was first added to each of the 100 mL polypropylene bottles, and then 100 mL of HNO_3 solution (pH = 2.00), ultrapure water (pH = 5.60), or NaOH solution (pH = 9.00) was added. After that, all the bottles were capped and soaked in three water baths with different constant temperatures (25°C, 35°C, or 45°C). From each bottle, the aqueous solutions (5 mL) were sampled at 22 time intervals (1, 3, 6, 12, 24, 48, 72, 120, 240, 360, 480, 720, 1080, 1440, 1800, 2160, 2880, 3600, 4320, 5040, 5760, and 7200 hours), filtered through 0.22 μm pore filters, and stabilized in 25 mL volumetric flask using 0.2% HNO_3. After each sampling, an equivalent volume of ultrapure water was supplemented. The aqueous Pb and P concentrations were determined by the ICP-OES. After 7200 h dissolution, the hydroxypyromorphite solids were sampled out of the bottles, rinsed, dried, and examined using the XRD, FT-IR, and FE-SEM.

2.3. Thermodynamic Calculations. The aqueous activities of $Pb^{2+}(aq)$, $PO_4^{3-}(aq)$, and $OH^-(aq)$ were first calculated using PHREEQC Version 3 with the minteq.v4.dat and llnl.dat databases [26], and then the ion activity products (IAPs) for $Pb_5(PO_4)_3OH$ were determined according to the mass-action expressions. The aqueous species considered for the total lead calculation included Pb^{2+}, $PbOH^+$, $Pb(OH)_2^0$, $Pb(OH)_3^-$, $Pb(OH)_4^{2-}$, Pb_2OH^{3+}, $Pb_4(OH)_4^{4+}$, $PbHPO_4^0$, $PbH_2PO_4^+$, and $PbP_2O_7^{2-}$. For the total phosphate, the species considered were PO_4^{3-}, HPO_4^{2-}, $H_2PO_4^-$, $H_3PO_4^0$, $PbHPO_4^0$, $PbH_2PO_4^+$, and $PbP_2O_7^{2-}$.

3. Results and Discussion

3.1. Solid Characterizations. The chemical composition of the synthetic lead hydroxypyromorphite [$Pb_5(PO_4)_3OH$] is dependent on the Pb/P molar ratio of the precursor solutions. The Pb-HAP precipitation should be conducted by mixing the lead solution with the phosphate solution very slowly. The obtained crystal was proved to be the intended component of $Pb_5(PO_4)_3OH$ with the atomic Pb/P ratio of 1.67. The obtained crystal was proved to be the intended component of $Pb_5(PO_4)_3OH$ with the atomic Pb/P ratio of 1.67, which decreased to 1.43~1.50, 1.58, and 1.58 after the dissolution at initial pH values 2.00, 5.60, and 9.00, respectively. As illustrated in the XRD, FT-IR, and FE-SEM figures, the component and characteristics of the Pb-HAP solids were almost indistinguishable before and after the dissolution at different initial pH values and 25°C (Figures 1–3). No secondary precipitates had been identified in the experiment at different initial pH values and 25°C. The XRD patterns of the hydroxypyromorphite solids showed that all the samples were recognized as lead phosphate hydroxide (reference code 01-087-2477), which were well crystallized and showed the apatite structure of the hexagonal system $P6_3/m$ with the estimated lattice parameters of $a = 0.989$ nm and $c = 0.748$ nm (Figure 1). But after the dissolution at initial pH 2.00 and 35°C (Figure 1(c)) or at initial pH 2.00 and 45°C (Figure 1(d)), the peaks of $Pb_3(PO_4)_2$ [lead phosphate, reference code 00-025-1394] were also recognized, which means that $Pb_3(PO_4)_2$ as secondary precipitate formed during the Pb-HAP dissolution at higher temperature. In the FT-IR spectra of

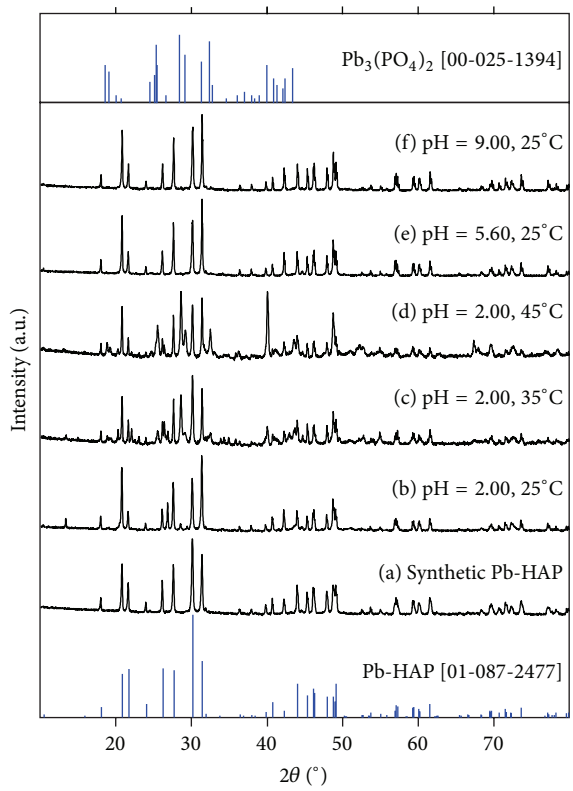

Figure 1: X-ray diffraction (XRD) patterns of the synthetic lead hydroxypyromorphite [$Pb_5(PO_4)_3OH$] before (a) and after (b–f) dissolution at 25–45°C for 300 d.

the hydroxypyromorphite solids (Figure 2), the normal vibrational modes of phosphate tetrahedra of lead hydroxypyromorphite (Pb-HAP) were witnessed within the range around at 938.24 cm^{-1} (ν_2), 985.01 and 1031.77 cm^{-1} (ν_3), and 536.62~573.74 cm^{-1} (ν_4). The phosphate peak at 471.53 cm^{-1} (ν_1) was not observed. The FT-IR spectra of all hydroxypyromorphite solids showed the very sharp bands at 3553.83 cm^{-1} for the stretching vibrations of the bulk OH^-. The 668.72 cm^{-1} bands represented the vibrational motion of OH^- [9]. The bands at 3650~3680 cm^{-1} for the surface P–OH groups [9] and the bands at 1455 cm^{-1} for the CO_3^{2-} vibration [28] were also not identified in the spectra. The band at 871 cm^{-1}, which was assigned to HPO_4^{2-} ions present in cation-deficient hydroxyapatite, was not detected in the spectra [9]. The FE-SEM results (Figure 3) confirmed that all hydroxypyromorphite solids were the typical hexagonal columnar crystals with a pinacoid as a termination, which elongated along the *c* axis. The mean particle length and width of Pb-HAP were obtained to be 7.00 μm (3.43~10.43 μm) and 3.76 μm (1.83~4.88) before dissolution, while these were 6.85 μm (3.81~11.87 μm) and 4.04 μm (2.96~5.14 μm), 5.49 μm (2.72~10.06 μm) and 3.44 μm (2.34~5.58 μm), and 5.62 μm (2.54~10.44 μm) and 3.55 μm (2.22~4.99 μm) after the dissolution at the initial pH values 2.00, 5.60, and 9.00, respectively.

3.2. Dissolution Mechanism. The solution element concentrations and ratios for the lead hydroxypyromorphite (Pb-HAP) dissolution at different pH values and temperatures versus time are showed in Figures 4(a)~4(f).

Dissolution of lead hydroxypyromorphite (Pb-HAP) at initial pH 2.00 appeared to be nearly stoichiometric in the early period and then nonstoichiometric to the end of the dissolution experiments. For the hydroxypyromorphite dissolution at initial pH 2.00 and 25°C (Figure 4(a)), the solution lead concentration rose continuously and reached a stable state after 720 h. The phosphate was rapidly released and the peak solution concentration was reached within the first hour of dissolution, and then the aqueous phosphate concentration decreased and reached a stable state after 720 h. The solution pH rose from 2.00 to 2.96 within 360 hours of the dissolution and then varied between 2.58 and 3.16 (Figure 4(a)). In addition, the release of lead and phosphate from solid to solution could be affected by the dissolution temperature. After dissolution for 7200 h, the solution phosphate concentrations at 45°C were lower than those at 25°C, while the solution lead concentrations at 45°C were higher than those at 25°C (Figures 4(a), 4(b), and 4(c)). The hydroxypyromorphite solids dissolved slowly while the solution Pb/P molar ratios increased constantly from 1.10–1.65 near the stoichiometric ratio of 1.67 to 210, 554, and 598 for the dissolution at initial pH 2.00 and 25°C, 35°C, and 45°C, respectively (Figure 4(f)).

Within the first 12 hours of the hydroxypyromorphite dissolution, lead and phosphate were released from the hydroxypyromorphite solid surface to the aqueous solution according to the stoichiometric Pb/P ratio of 1.67 (Figure 4(f)). The aqueous Pb/P molar ratio increased with the time increasing, which showed that the lead ions were preferentially released from the solid surface in comparison with phosphate. At the end of our experiment (7200 h), the solution Pb/P molar ratios were 74.76, 86.15, and 237.26 for the hydroxypyromorphite dissolution at initial pH 2.00 and 25°C, 35°C, and 45°C, respectively (Figure 4(f)). The aqueous Pb/P molar ratios for the dissolution at 45°C were considerably greater than the values at 25°C, which showed that the solution temperature could noticeably affect the solubility and dissolution mechanism of hydroxypyromorphite. As indicated in Figures 1(c) and 1(d), the surface phase of the lead hydroxypyromorphite particles dissolved under pH 2.00 and 35°C or initial pH 2.00 and 45°C condition, and $Pb_3(PO_4)_2$ phase with the Pb/P molar ratio of 1.50 was formed on the surface of the particle. Moreover, some Pb^{2+} sites in the lead hydroxypyromorphite structure are possibly vacant [20]. Consequently the excess Pb^{2+} ions were released to the solution.

For the hydroxypyromorphite dissolution in pure water (pH = 5.60) and the solution of initial pH 9.00, the solution pH values, lead and phosphate concentrations reached a stable state after 2880 h, which indicated a possible attainment of a steady state between the hydroxypyromorphite solid and the aqueous solution (Figures 4(d) and 4(e)). The solution lead and phosphate concentrations decreased with the increasing solution pH values.

With the early release of Pb^{2+} and PO_4^{3-} into the alkaline solution was the rapid rising of the solution pH from 9.00 to 9.72 within the 1 h dissolution, and then the solution pH values declined and attained a stable state with the pH values

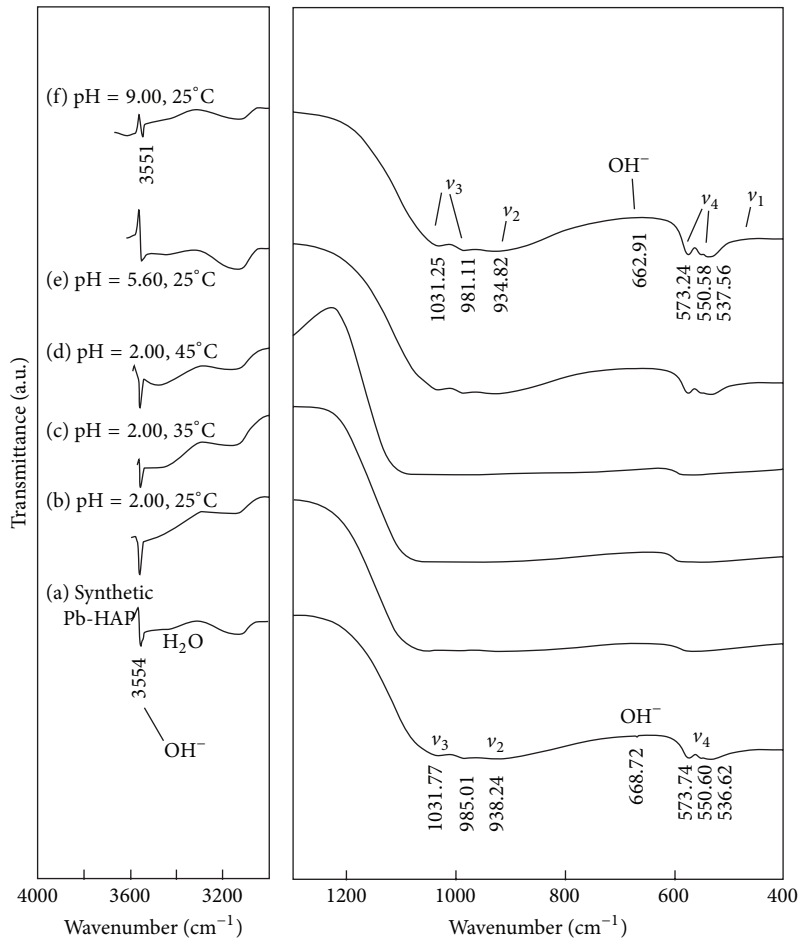

Figure 2: Fourier transform infrared (FT-IR) spectra of the synthetic lead hydroxypyromorphite [$Pb_5(PO_4)_3OH$] before (a) and after (b–f) dissolution at 25–45°C for 300 d.

of about 6.19~6.40 after dissolution for 120 h. For the dissolution at initial pH 2.00 or 5.60, all solution pH values were higher than the initial pH values. The H^+ consuming showed that the H^+ adsorption onto negatively charged oxygen ions of phosphate groups of lead hydroxypyromorphite (Pb-HAP) may result in the transforming of PO_4^{3-} into HPO_4^{2-} at the solid surface and promote the dissolution process. In addition, the coexistence of dissolution and exchange processes indicated that the H^+ ions depleted during the hydroxypyromorphite dissolution were derived not only from the H^+ sorption/desorption reactions but also from various processes at the hydroxypyromorphite surface. As a result, a comprehensive elucidation of the H^+ consuming during the dissolution should cover all the following reactions: stoichiometric dissolution of the bulk hydroxypyromorphite solid, stoichiometric exchange of $2H^+$ for one Pb^{2+} at the hydroxypyromorphite surface, and H^+ adsorption/desorption at the hydroxypyromorphite surface [20, 29]. The apatite dissolution mechanism is particularly dependent on the experimental conditions [20]. Many models for the apatite dissolution have been proposed depending upon the available experimental results, but all of them take only certain aspects of the apatite dissolution into consideration and cannot describe the dissolution mechanism completely [20].

Depending upon the experimental results of earlier researches [20] and this work, the lead hydroxypyromorphite (Pb-HAP) dissolution in water is thought to include the following steps or processes: (I) stoichiometric dissolution coupled with protonation and complexation reactions; (II) nonstoichiometric dissolution with Pb^{2+} release and PO_4^{3-} sorption; (III) sorption of Pb^{2+} and PO_4^{3-} species from solution backwards onto Pb-HAP surface; (IV) stable state.

In Process I, for the hydroxypyromorphite dissolution in solution at initial pH 2.00 and 25°C, Pb^{2+} and PO_4^{3-} in the hydroxypyromorphite structure can be released from solid to solution stoichiometrically according to reaction (1); the solution lead and phosphate concentrations rose with time simultaneously with the solution Pb/P molar ratio of 1.67 at the early stage of hydroxypyromorphite dissolution (0~120 h). Various probable reactions should be taken into account in the apatite dissolution because of its complicated structure [30]. Reaction (1) for the lead hydroxypyromorphite

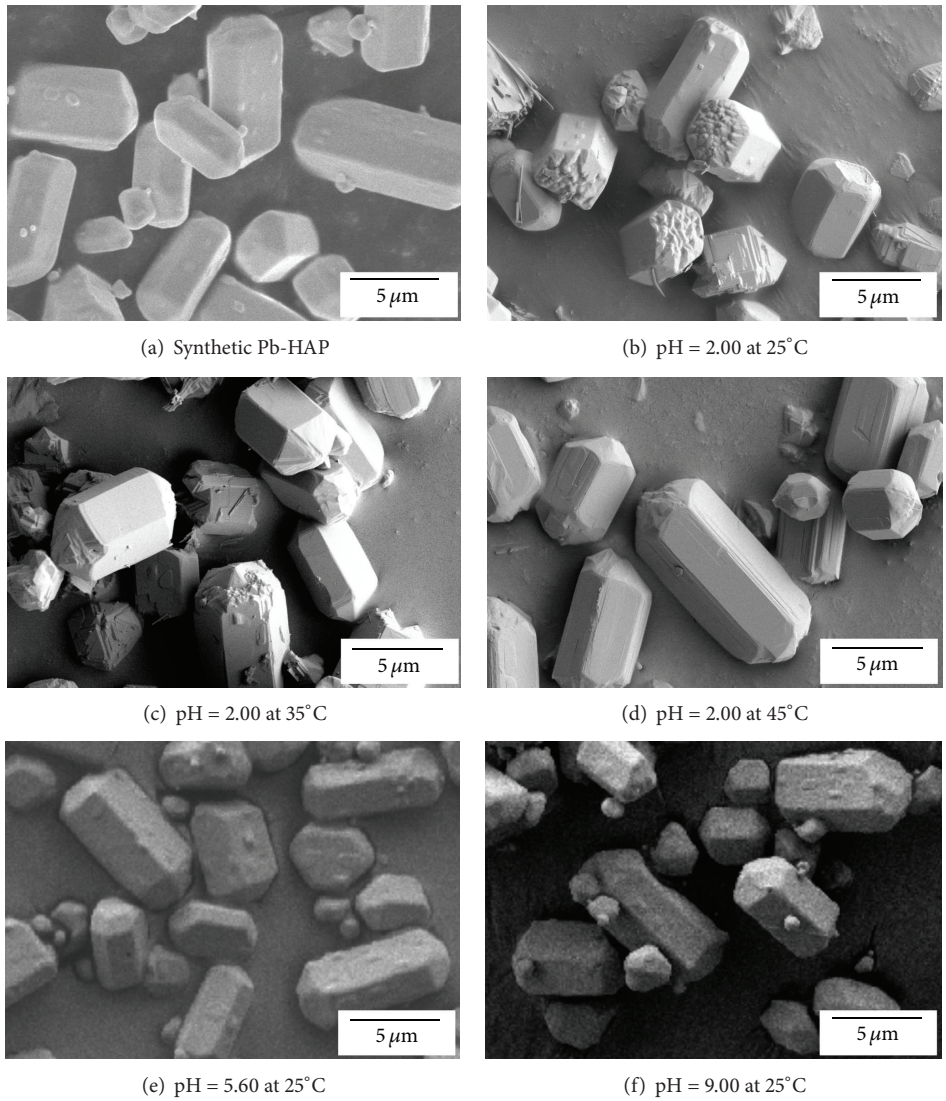

(a) Synthetic Pb-HAP (b) pH = 2.00 at 25°C

(c) pH = 2.00 at 35°C (d) pH = 2.00 at 45°C

(e) pH = 5.60 at 25°C (f) pH = 9.00 at 25°C

FIGURE 3: Field emission-scanning electron microscopy (FE-SEM) images of the synthetic lead hydroxypyromorphite [$Pb_5(PO_4)_3OH$] before (a) and after (b–f) dissolution at 25–45°C for 300 d.

dissolution can be considerably affected by the solution pH and coupled with protonation and complexation reactions (2), (3), and (4), which caused the increasing of the solution pH for the hydroxypyromorphite dissolution in aqueous acidic media or the decreasing of the solution pH for the hydroxypyromorphite dissolution in aqueous alkali media. Consider

$$Pb_5(PO_4)_3OH \longleftrightarrow 5Pb^{2+} + 3PO_4^{3-} + OH^- \quad (1)$$

$$PO_4^{3-} + nH^+ \longleftrightarrow H_nPO_4^{(3-n)-} \quad (n = 1, 2, 3) \quad (2)$$

$$Pb^{2+} + nOH^- \longleftrightarrow Pb(OH)_n^{(n-2)-} \quad (n = 1, 2, 3, 4) \quad (3)$$

$$Pb^{2+} + H_nPO_4^{(3-n)-} \longleftrightarrow PbH_nPO_4^{(n-1)+} \quad (n = 1, 2). \quad (4)$$

The lead and phosphate speciation results based on the simulation with PHREEQC showed that, for the hydroxypyromorphite (Pb-HAP) dissolution at initial pH 2.00 and 25°C, the solution lead species existed in the order of Pb^{2+} > $PbOH^+$ > $PbHPO_4^0$ ≫ $PbH_2PO_4^+$ > $Pb(OH)_2$ ≫ $Pb(OH)_3^-$ ≫ $Pb(OH)_4^{2-}$; the solution phosphate species occurred in the order of $H_2PO_4^-$ > H_3PO_4 ≫ $PbHPO_4^0$ > HPO_4^{2-} ≫ $PbH_2PO_4^+$ ≫ PO_4^{3-}. At the early stage of the Pb-HAP dissolution at initial pH 9.00 and 25°C, the solution lead species existed in the order of $PbOH^+$ > $Pb(OH)_2$ > $Pb(OH)_3^-$ > Pb^{2+} ≫ $Pb(OH)_4^{2-}$ > $PbHPO_4^0$ ≫ $PbH_2PO_4^+$; the solution phosphate species occurred in the order of HPO_4^{2-} > $H_2PO_4^-$, PO_4^{3-} > $PbHPO_4^0$ ≫ H_3PO_4 ≫ $PbH_2PO_4^+$. At the dissolution time >120 h, the solution lead species existed in the order of Pb^{2+} > $PbOH^+$ > $PbHPO_4^0$ > $Pb(OH)_2$ > $Pb(OH)_3^-$ > $PbH_2PO_4^+$ > $Pb(OH)_4^{2-}$; the solution phosphate species occurred in

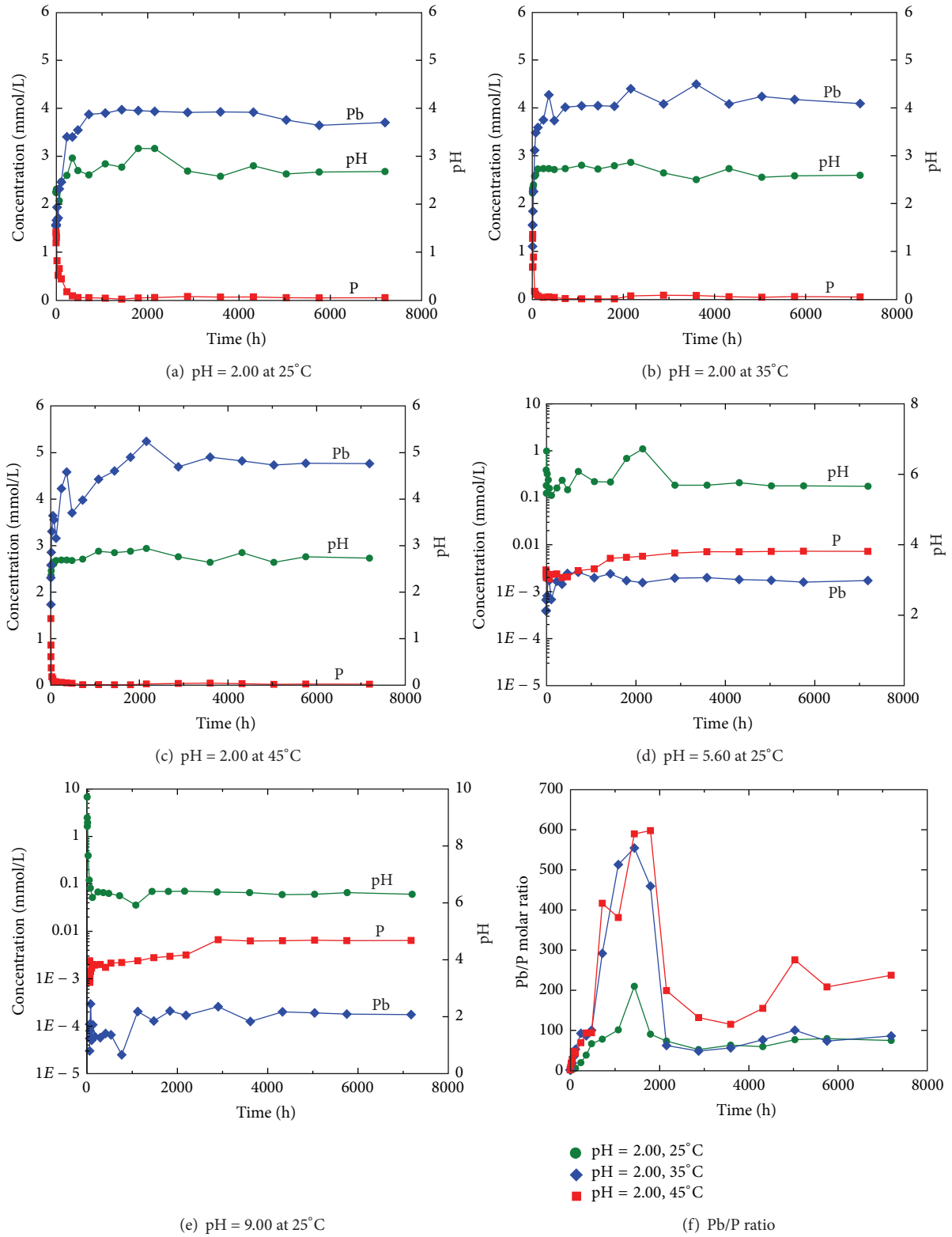

Figure 4: Aqueous evolution during the dissolution of the synthetic lead hydroxypyromorphite [$Pb_5(PO_4)_3OH$] at 25–45°C for 300 d.

the order of $H_2PO_4^- > HPO_4^{2-} \gg H_3PO_4 > PbHPO_4^0 \gg PO_4^{3-} \gg PbH_2PO_4^+$.

In Process II, lead and phosphate were removed nonstoichiometrically from the hydroxypyromorphite structure with the solution Pb/P molar ratio > 1.67. Consequently, a surface layer, which had a chemical composition different from that of the bulk solid, could be formed [20]. After a first portion of the hydroxypyromorphite had been dissolved, some phosphate species could be adsorbed from the solution backwards onto the hydroxypyromorphite surface. The aqueous phosphate concentration started to decrease progressively after 1 h dissolution at initial pH 2.00 and 25°C, whereas the solution lead concentration rose continuously with time. The solution Pb/P molar ratio increased from about 1.67 to 209.85 after 1440 h dissolution.

In Process III, both of lead and phosphate species were adsorbed at the same time from the solution backwards onto the hydroxypyromorphite surface; the solution lead and phosphate concentrations declined from 1440 h to 5040 h with the decreasing solution Pb/P molar ratio (209.85 to 76.74), which might lead to the formation of a solid surface layer with a composition differing from the bulk of hydroxypyromorphite [20]; that is, the final solution reached a stable state with the solid surface layer having a composition different from hydroxypyromorphite $[Pb_5(PO_4)_3OH]$. Because of the very low solubility, it was proposed that the apatite dissolution at the atomic level was ever nonstoichiometric [20], and its mechanism might include several chemical reactions taking place simultaneously at the apatite surface [30, 31].

In Process IV, desorption and adsorption of lead and phosphate species attained a stable state. The solution lead and phosphate concentrations were nearly constant for the hydroxypyromorphite dissolution in the acidic solution (pH 2.00) at 25°C from 5040 h to 7200 h in the present work, and the solution Pb/P molar ratios were 74.76~79.59.

3.3. Determination of Solubility. The solubility product (K_{sp}) for lead hydroxypyromorphite $[Pb_5(PO_4)_3OH]$ was determined by using the activities of the solution lead and phosphate species in the final equilibrated solutions (5040 h, 5760 h, and 7200 h). The aqueous solutions were undersaturated with respect to any possible secondary minerals (e.g., massicot (PbO), litharge (PbO), $PbO{\cdot}0.3H_2O$, plattnerite (PbO_2), $Pb(OH)_2$, $Pb_2O(OH)_2$, $PbHPO_4$, and $Pb_3(PO_4)_2$).

The dissolution of lead hydroxypyromorphite and the release of lead and phosphate can be expressed by the dissolution reaction (1). Assuming unit activity of the solid phase

$$K_{sp} = \left\{Pb^{2+}\right\}^5 \left\{PO_4^{3-}\right\}^3 \left\{OH^-\right\}, \quad (5)$$

where K_{sp} is the equilibrium constant of dissolution reaction (1) and {} represents the thermodynamic activities of the solution species.

The standard free energy of reaction (ΔG_r^o), in kJ/mol, depends upon the solubility product (K_{sp}) under the standard condition (298.15 K and 0.101 MPa) by

$$\Delta G_r^o = -5.708 \log K_{sp}. \quad (6)$$

For (1),

$$\Delta G_r^o = 5\Delta G_f^o\left[Pb^{2+}\right] + 3\Delta G_f^o\left[PO_4^{3-}\right] + \Delta G_f^o\left[OH^-\right] - \Delta G_f^o\left[Pb_5(PO_4)_3OH\right]. \quad (7)$$

Rearranging,

$$\Delta G_f^o\left[Pb_5(PO_4)_3OH\right] = 5\Delta G_f^o\left[Pb^{2+}\right] + 3\Delta G_f^o\left[PO_4^{3-}\right] + \Delta G_f^o\left[OH^-\right] - \Delta G_r^o. \quad (8)$$

Table 1 lists the pH, Pb, and P analyses at different initial solution pH values and temperatures, as well as the calculated solubility products (K_{sp}) for lead hydroxypyromorphite $[Pb_5(PO_4)_3OH]$. The aqueous activities of Pb^{2+}(aq), PO_4^{3-}(aq), and OH^-(aq) were first calculated via the computer program PHREEQC [26], and then the K_{sp} values for hydroxypyromorphite $[Pb_5(PO_4)_3OH]$ were calculated according to (5). The average K_{sp} values were calculated for hydroxypyromorphite $[Pb_5(PO_4)_3OH]$ of $10^{-80.77}$ ($10^{-80.57}$–$10^{-80.96}$) at 25°C, $10^{-80.65}$ ($10^{-80.38}$–$10^{-80.99}$) at 35°C, and $10^{-79.96}$ ($10^{-79.38}$–$10^{-80.71}$) at 45°C, which may be compared with the reported constant for lead chloropyromorphite $[Pb_5(PO_4)_3Cl]$ of $10^{-83.61}$ [16].

Based on the determined solubility data from the dissolution at initial pH 2.00 and 25°C, the Gibbs free energy of formation [ΔG_f^o] for hydroxypyromorphite $[Pb_5(PO_4)_3OH]$ was calculated using (6), (7), and (8) to be −3796.71 kJ/mol (−3795.55~ −3797.78 kJ/mol); a lower value than −3773.968 kJ/mol corresponds to a K_{sp} of $10^{-76.8}$ for hydroxypyromorphite $[Pb_5(PO_4)_3OH]$ [24, 25].

The average K_{sp} values were determined for Ca-HAP $[Ca_5(PO_4)_3OH]$ and Cd-HAP $[Cd_5(PO_4)_3OH]$ of $10^{-58.38}$ ($10^{-58.31}$–$10^{-58.46}$) and $10^{-64.62}$ ($10^{-64.53}$–$10^{-64.71}$) at 25°C in our study. The thermodynamic solubility products (K_{sp}) for Ca-HAP $[Ca_5(PO_4)_3OH]$ were reported to be $10^{-58.3}$ [32], 10^{-57} [33], 10^{-59} [34], $10^{-58\pm1}$ [18], and $10^{-57.72}$ [35]. In comparison with the solubility products for Ca-HAP in literature, the average K_{sp} value $10^{-80.77}$ for Pb-HAP was nearly 23.77–21.77 log units lesser than 10^{-57}–10^{-59} for Ca-HAP. The solubility product for Pb-HAP is extremely low, that is, several orders of magnitude less soluble than Ca-HAP. Comparison of the solubility products (K_{sp}) for calcium hydroxyapatite (Ca-HAP) and lead hydroxypyromorphite (Pb-HAP) shows that the conversion of Ca-HAP to Pb-HAP is thermodynamically favorable in the presence of aqueous Pb^{2+} [36].

The solubility products (K_{sp}) obtained in this and earlier researches [24, 25] indicate the stability sequence for the hydroxyapatites to be Pb-HAP ≫ Cd-HAP > Ca-HAP, which may be related with the crystal radii for Pb^{2+}, Cd^{2+}, and Ca^{2+} of 0.119 nm, 0.095 nm, and 0.100 nm, respectively. Some workers have studied the influence of various phosphate amendments (synthetic hydroxyapatite, phosphate rock, calcium hydrogen phosphate, phosphoric acid, and phosphate

Table 1: Analytical data and solubility determination of lead hydroxypyromorphite [$Pb_5(PO_4)_3OH$].

Temp	Initial pH	Reaction time (hours)	Analytical data			$\log K_{sp}$	ΔG_f^o [kJ/mol]
			pH	Pb (mmol/L)	P (mmol/L)		
25°C	2.00	5040	2.63	3.76	0.0489	−80.96	−3797.78
		5760	2.67	3.64	0.0458	−80.79	−3796.79
		7200	2.68	3.70	0.0495	−80.57	−3795.55
35°C	2.00	5040	2.55	4.24	0.0422	−80.99	
		5760	2.58	4.17	0.0569	−80.38	
		7200	2.59	4.09	0.0475	−80.57	
45°C	2.00	5040	2.64	4.73	0.0172	−80.71	
		5760	2.76	4.77	0.0229	−79.38	
		7200	2.73	4.76	0.0201	−79.78	
25°C	5.60	5040	0.58	0.00175	0.00720	−77.42	−3777.57
		5760	0.34	0.00160	0.00726	−77.60	−3778.61
		7200	0.17	0.00173	0.00723	−77.51	−3778.06
25°C	9.00	5040	6.30	0.000191	0.00649	−78.17	−3781.84
		5760	6.36	0.000180	0.00636	−77.94	−3780.54
		7200	6.30	0.000175	0.00642	−78.37	−3782.97

fertilizers) and suggested that the precipitation of the lead-bearing hydroxypyromorphite results from earlier dissolution of calcium hydroxyapatite, which is much more soluble than lead hydroxypyromorphite [16]. Continuous dissolution of calcium hydroxyapatite was detected as the result of the formation of less soluble lead hydroxypyromorphite [16]. The transport-controlled calcium hydroxyapatite dissolution provided phosphate for precipitation of lead hydroxypyromorphite [$Pb_5(PO_4)_3OH$], which in turn sequestered solution Pb^{2+} [36].

4. Conclusions

The synthetic solid was pure lead hydroxypyromorphite (Pb-HAP) with the crystal lattice parameters of $a = 0.989$ nm and $c = 0.748$ nm. The normal vibrational modes of phosphate tetrahedra for hydroxypyromorphite were observed around 938.24 cm^{-1} (ν_2), 985.01 and 1031.77 cm^{-1} (ν_3), and 536.62~573.74 cm^{-1} (ν_4). The hydroxypyromorphite solid was the typical hexagonal columnar crystals with pinacoids as the termination that elongated along the c axis (particle sizes 2~20 μm). The XRD, FT-IR, and FE-SEM results indicated that the hydroxypyromorphite solids had no obvious change during dissolution.

For the hydroxypyromorphite dissolution in acidic solution (initial pH 2.00) at 25°C, the solution phosphate concentrations rose quickly and attained the peak value after 1 h dissolution, while the aqueous lead concentrations rose slowly and attained the peak value after 1440 h. The solution Pb/P molar ratio increased constantly from 1.10~1.65 near the stoichiometric ratio of 1.67 to 209.85~597.72 and then decreased to 74.76~237.26 for the dissolution at initial pH 2.00 and 25°C~45°C. The average solubility products (K_{sp}) for hydroxypyromorphite [$Pb_5(PO_4)_3OH$] were determined to be $10^{-80.77}$ ($10^{-80.57}$–$10^{-80.96}$) at 25°C, $10^{-80.65}$ ($10^{-80.38}$–$10^{-80.99}$) at 35°C, and $10^{-79.96}$ ($10^{-79.38}$–$10^{-80.71}$) at 45°C. From the obtained solubility data for the dissolution at initial pH 2.00 and 25°C, the Gibbs free energy of formation [ΔG_f^o] for $Pb_5(PO_4)_3OH$ was calculated to be −3796.71 kJ/mol (−3795.55~ −3797.78 kJ/mol). According to these constants, the stability sequence for hydroxyapatite is Pb-HAP > Cd-HAP > Ca-HAP.

Conflict of Interests

The authors declare that there is no conflict of interests regarding the publication of this paper.

Acknowledgments

The paper has greatly benefited from insightful comments by the editor and anonymous reviewers. This research was financially assisted by the National Natural Science Foundation of China (NSFC41263009), the Guangxi Science and Technology Development Project (GuiKeGong14124004-3-3, GuiKeZhong1298002-3), the Provincial Natural Science Foundation of Guangxi (2012GXNSFDA053022), and the Project of High Level Innovation Team and Outstanding Scholar in Guangxi Colleges and Universities (no. 002401013001).

References

[1] A. Yasukawa, K. Kamiuchi, T. Yokoyama, and T. Ishikawa, "Preparation of lead-calcium hydroxyapatite solid solutions by a wet method using acetamide," *Journal of Solid State Chemistry*, vol. 163, no. 1, pp. 27–32, 2002.

[2] K. Zhu, K. Yanagisawa, A. Onda, K. Kajiyoshi, and J. Qiu, "Morphology variation of cadmium hydroxyapatite synthesized by high temperature mixing method under hydrothermal conditions," *Materials Chemistry and Physics*, vol. 113, no. 1, pp. 239–243, 2009.

[3] K. Zhu, J. Qiu, H. Ji et al., "Crystallographic study of lead-substituted hydroxyapatite synthesized by high-temperature mixing method under hydrothermal conditions," *Inorganica Chimica Acta*, vol. 363, no. 8, pp. 1785–1790, 2010.

[4] B. Orzechowska-Wylęgała, A. Obuchowicz, P. Malara, A. Fischer, and B. Kalita, "Cadmium and lead accumulate in the deciduous teeth of children with celiac disease or food allergies," *International Journal of Stomatology & Occlusion Medicine*, vol. 4, no. 1, pp. 28–31, 2011.

[5] E. Ghomash Pasand, A. Nemati, M. Solati-Hashjin, K. Arzani, and A. Farzadi, "Microwave assisted synthesis & properties of nano HA-TCP biphasic calcium phosphate," *International Journal of Minerals, Metallurgy and Materials*, vol. 19, no. 5, pp. 441–445, 2012.

[6] M. Zakeri, E. Hasani, and M. Tamizifar, "Mechanical properties of TiO_2-hydroxyapatite nanostructured coatings on Ti-6Al-4V substrates by APS method," *International Journal of Minerals, Metallurgy and Materials*, vol. 20, no. 4, pp. 397–402, 2013.

[7] A. B. Cherifa, M. Jemal, A. Nounah, and J. L. Lacout, "Enthalpy of formation and enthalpy of mixing of calcium and cadmium hydroxyapatites," *Thermochimica Acta*, vol. 237, no. 2, pp. 285–293, 1994.

[8] P. P. Mahapatra, D. S. Sarangi, and B. Mishra, "Kinetics of nucleation of lead hydroxylapatite and preparation of solid solutions of calcium-cadmium-lead hydroxylapatite: an X-ray and IR study," *Journal of Solid State Chemistry*, vol. 116, no. 1, pp. 8–14, 1995.

[9] A. Yasukawa, M. Higashijima, K. Kandori, and T. Ishikawa, "Preparation and characterization of cadmium-calcium hydroxyapatite solid solution particles," *Colloids and Surfaces A: Physicochemical and Engineering Aspects*, vol. 268, no. 1–3, pp. 111–117, 2005.

[10] C. Piccirillo, S. I. A. Pereira, A. P. G. C. Marques et al., "Bacteria immobilisation on hydroxyapatite surface for heavy metals removal," *Journal of Environmental Management*, vol. 121, pp. 87–95, 2013.

[11] Z. Evis, B. Yilmaz, M. Usta, and S. L. Aktug, "X-ray investigation of sintered cadmium doped hydroxyapatites," *Ceramics International*, vol. 39, no. 3, pp. 2359–2363, 2013.

[12] N. Arnich, M.-C. Lanhers, F. Laurensot, R. Podor, A. Montiel, and D. Burnel, "In vitro and in vivo studies of lead immobilization by synthetic hydroxyapatite," *Environmental Pollution*, vol. 124, no. 1, pp. 139–149, 2003.

[13] S. Bailliez, A. Nzihou, E. Bèche, and G. Flamant, "Removal of lead (Pb) by hydroxyapatite sorbent," *Process Safety and Environmental Protection*, vol. 82, no. 2, pp. 175–180, 2004.

[14] S. H. Jang, Y. G. Jeong, B. G. Min, W. S. Lyoo, and S. C. Lee, "Preparation and lead ion removal property of hydroxyapatite/polyacrylamide composite hydrogels," *Journal of Hazardous Materials*, vol. 159, no. 2-3, pp. 294–299, 2008.

[15] L. Dong, Z. Zhu, Y. Qiu, and J. Zhao, "Removal of lead from aqueous solution by hydroxyapatite/magnetite composite adsorbent," *Chemical Engineering Journal*, vol. 165, no. 3, pp. 827–834, 2010.

[16] M. C. F. Magalhães and P. A. Williams, "Apatite group minerals: solubility and environmental remediation," in *Thermodynamics, Solubility and Environmental Issues*, T. M. Letcher, Ed., pp. 327–340, Elsevier, Amsterdam, The Netherlands, 2007.

[17] A. Xenidis, C. Stouraiti, and N. Papassiopi, "Stabilization of Pb and As in soils by applying combined treatment with phosphates and ferrous iron," *Journal of Hazardous Materials*, vol. 177, no. 1–3, pp. 929–937, 2010.

[18] E. Valsami-Jones, K. V. Rggnarsdottir, A. Putnis, D. Bosbach, A. J. Kemp, and G. Cressey, "The dissolution of apatite in the presence of aqueous metal cations at pH 2-7," *Chemical Geology*, vol. 151, no. 1-4, pp. 215–233, 1998.

[19] M. T. Fulmer, I. C. Ison, C. R. Hankermayer, B. R. Constantz, and J. Ross, "Measurements of the solubilities and dissolution rates of several hydroxyapatites," *Biomaterials*, vol. 23, no. 3, pp. 751–755, 2002.

[20] S. V. Dorozhkin, "A review on the dissolution models of calcium apatites," *Progress in Crystal Growth and Characterization of Materials*, vol. 44, no. 1, pp. 45–61, 2002.

[21] W.-J. Tseng, C.-C. Lin, and P.-W. Shen, "Directional/acidic dissolution kinetics of (OH,F,Cl)-bearing apatite," *Journal of Biomedical Materials Research Part A*, vol. 76, no. 4, pp. 753–764, 2006.

[22] N. Harouiya, C. Chaïrat, S. J. Köhler, R. Gout, and E. H. Oelkers, "The dissolution kinetics and apparent solubility of natural apatite in closed reactors at temperatures from 5 to 50°C and pH from 1 to 6," *Chemical Geology*, vol. 244, no. 3-4, pp. 554–568, 2007.

[23] K. Skartsila and N. Spanos, "Surface characterization of hydroxyapatite: potentiometric titrations coupled with solubility measurements," *Journal of Colloid and Interface Science*, vol. 308, no. 2, pp. 405–412, 2007.

[24] J. O. Nriagu, "Lead orthophosphates. I. Solubility and hydrolysis of secondary lead orthophosphate," *Inorganic Chemistry*, vol. 11, no. 10, pp. 2499–2503, 1972.

[25] J. O. Nriagu, "Lead orthophosphates-IV formation and stability in the environment," *Geochimica et Cosmochimica Acta*, vol. 38, no. 6, pp. 887–898, 1974.

[26] D. L. Parkhurst and C. A. J. Appelo, "Description of input and examples for PHREEQC version 3—a computer program for speciation, batch-reaction, one-dimensional transport, and inverse geochemical calculations," in *U.S. Geological Survey Techniques and Methods*, Book 6, chapter A43, pp. 1–497, 2013.

[27] X. Zhao, Y. Zhu, and L. Dai, "Synthesis and characterization of cadmium-calcium hydroxyapatite solid solutions," *International Journal of Minerals, Metallurgy, and Materials*, vol. 21, no. 6, pp. 604–608, 2014.

[28] G.-R. Qian, H.-M. Bai, F.-C. Sun, J.-Z. Zhou, W.-M. Sun, and X. Xu, "Preparation and stability of calcium cadmium hydroxyapatite," *Journal of Inorganic Materials*, vol. 23, no. 5, pp. 1016–1020, 2008 (Chinese).

[29] C. Chaïrat, E. H. Oelkers, J. Schott, and J.-E. Lartigue, "Fluorapatite surface composition in aqueous solution deduced from potentiometric, electrokinetic, and solubility measurements, and spectroscopic observations," *Geochimica et Cosmochimica Acta*, vol. 71, no. 24, pp. 5888–5900, 2007.

[30] Å. Bengtsson, A. Shchukarev, P. Persson, and S. Sjöberg, "A solubility and surface complexation study of a non-stoichiometric hydroxyapatite," *Geochimica et Cosmochimica Acta*, vol. 73, no. 2, pp. 257–267, 2009.

[31] R. A. Berner, "Kinetics of weathering and diagenesis," *Reviews in Mineralogy and Geochemistry*, vol. 8, no. 1, pp. 111–134, 1981.

[32] H. McDowell, T. M. Gregory, and W. E. Brown, "Solubility of $Ca_5(PO_4)_3OH$ in the system $Ca(OH)_2$–H_3PO_4–H_2O at 5, 15, 25, and 37°C," *Journal of Research of the National Bureau of Standards—A: Physics and Chemistry*, vol. 81, no. 2-3, pp. 273–281, 1977.

[33] W. Stumm and J. J. Morgan, *Aquatic Chemistry, Chemical Equilibria and Rates in Natural Waters*, John Wiley & Sons, New York, NY, USA, 1996.

[34] W. E. Brown, T. M. Gregory, and L. C. Chow, "Effects of fluoride on enamel solubility and cariostasis," *Caries Research*, vol. 11, supplement 1, pp. 118–141, 1977.

[35] C. Wei, Y. Zhu, F. Yang, J. Li, Z. Zhu, and H. Zhu, "Dissolution and solubility of hydroxylapatite and fluorapatite at 25°C at different pH," *Research Journal of Chemistry and Environment*, vol. 17, no. 11, pp. 57–61, 2013.

[36] S. K. Lower, P. A. Maurice, and S. J. Traina, "Simultaneous dissolution of hydroxylapatite and precipitation of hydroxypyromorphite: direct evidence of homogeneous nucleation," *Geochimica et Cosmochimica Acta*, vol. 62, no. 10, pp. 1773–1780, 1998.